Prediction of Water Solubility in Glassy Polymers Using Nonequilibrium Thermodynamics

ARTICLE *in* INDUSTRIAL & ENGINEERING CHEMISTRY RESEARCH · AUGUST 2013

Impact Factor: 2.59 · DOI: 10.1021/ie401713h

2 AUTHORS, INCLUDING:

Eric M. Davis
Clemson University
16 PUBLICATIONS **81** CITATIONS

SEE PROFILE

I&EC research
Industrial & Engineering Chemistry Research

Article

pubs.acs.org/IECR

Prediction of Water Solubility in Glassy Polymers Using Nonequilibrium Thermodynamics

Eric M. Davis and Yossef A. Elabd*

Department of Chemical and Biological Engineering, Drexel University, Philadelphia, Pennsylvania 19104, United States

Supporting Information

ABSTRACT: In this study, the sorption of water in poly(methyl methacrylate) (PMMA) was measured at various water vapor activities (0−0.85) at 25, 35, and 45 °C using a quartz spring microbalance. Furthermore, the water sorption isotherms in PMMA were predicted using two nonequilibrium thermodynamic models: the nonequilibrium lattice fluid (NELF) model and nonequilibrium statistical associating fluid theory (NE-SAFT), where excellent agreement between the NE-SAFT prediction and experimental data was observed. In contrast, deviation between the NELF model prediction and water sorption isotherms in PMMA was observed above a water activity of ca. 0.50. In situ time-resolved Fourier transform infrared attenuated total reflectance spectroscopy confirmed the presence of self-associated water (i.e., water clusters) at elevated water activities, providing a rationale for deviation between the NELF model and experimental data, where unlike NE-SAFT, the NELF model does not account for these self-association interactions. The NE-SAFT model prediction was extended to five additional glassy polymers, including poly(lactide), poly(acrylonitrile), poly(ethylene terephthalate), poly(vinyl chloride), and poly(styrene), where good agreement between the model predictions and water sorption isotherms was also observed. Additionally, a correlation between the polymer segment number and water solubility was observed.

INTRODUCTION

Water sorption and diffusion in polymers are important in many fields, including drug delivery,[1] desalination,[2,3] fuel cells,[4] flow batteries,[5] coatings,[6] and packaging.[7] Several factors must be considered for measuring the transport of small molecules (e.g., water) in polymers. Specifically, when the experimental temperature is below the glass transition temperature of the polymer (i.e., glassy polymer), the specific volume of the polymer is in a nonequilibrium state (i.e., time-dependent relaxation), and therefore the polymer can continually and gradually sorb more penetrant (water) long after the standard time scale for diffusion.[6,8−10] This time-dependent relaxation renders it difficult to accurately measure and/or predict the sorption of water in the polymer. The deviation from Fickian diffusion (i.e., anomalous transport) requires careful attention during measurement of water sorption and water sorption kinetics, where the relationship between the polymer film thickness and time of the experiment is critical in measuring reproducible solubility values and, ultimately, the solubility values used in comparison to those predicted from appropriate predictive models. To this end, the demonstration of predictive thermodynamic models that account for the nonequilibrium state of the glassy polymer can provide new insight into fundamental model parameters (e.g., polymer chain volume and number and water hydrogen bonding/self-association) and their impact on water solubility.

The investigation of water sorption and diffusion in polymers has increasingly gained attention because of its impact on a broad array of practical applications.[6,11−20] One example includes the work of Prausnitz and co-workers,[21,22] where they investigated the sorption and diffusion of water in several glassy polymers, including poly(methyl methacrylate) (PMMA), poly(acrylic acid), and poly(*N*-vinyl-2-pyrrolidone). With the use of the Flory−Huggins model, they regressed an "effective" χ value between water and the polymer from the experimental water sorption data. They used the results from this analysis in conjunction with predictions from the Zimm−Lundberg clustering function[23] to postulate that water exists as monomers (nonassociated molecules) in some glassy polymers and clusters (highly self-associated molecules) in others. The authors do acknowledge that the Flory−Huggins and Zimm−Lundberg models are derived under the framework of equilibrium thermodynamics. For the water/poly(*N*-vinyl-2-pyrrolidone) mixture, the glassy polymer sorbs enough water to lower its glass transition temperature (i.e., plasticize) below the experimental temperature; however, for other water/polymer mixtures (e.g., water/PMMA), the polymer sorbs a small amount of water (∼1.5 wt %), which has little impact on its high glass transition temperature. Regardless, this recent study highlights the importance of water clustering and how it could play a critical role in predicting water solubility in a polymer in a nonequilibrium state.

Recently, Davis et al.[24,25] investigated the nonequilibrium sorption and sorption kinetics of water in poly(lactide) (PLA), a glassy polymer synthesized from renewable sources. Non-Fickian kinetics, specifically two-stage sorption kinetics, was observed, where Fickian kinetics was observed in the first stage and additional water sorption was observed at later times. Furthermore, identical solubility values were obtained between multiple experimental techniques [e.g., quartz crystal microbalance (QCM) and quartz spring microbalance (QSM)] by

Received: May 29, 2013
Revised: August 9, 2013
Accepted: August 13, 2013
Published: August 13, 2013

dx.doi.org/10.1021/ie401713h | *Ind. Eng. Chem. Res.* 2013, 52, 12865−12875

comparing the solubility at the Fickian pseudoequilibrium state of the sorption kinetic data as a consistent reference at each step of the differential water sorption experiment. This work highlights the importance of the relationship between the glassy polymer film thickness and time of the experiment, where an infinite number of solubility values could be reported after the Fickian pseudoequilibrium of the water uptake kinetic data.

Typical thermodynamic models to predict the mixture composition, where one component is a polymer, such as the Flory–Huggins model,[26−29] often fail to adequately describe a mixture with a glassy polymer as the major component[30−32] because these models are constructed under the framework of equilibrium thermodynamics [i.e., temperatures, pressures, and component fugacities (or component excess Gibbs free energies) are set equal between the water vapor and condensed water–polymer phases], indicated by a concentration-dependent interaction parameter (χ).[33] To account for the nonequilibrium behavior observed in the sorption data of glassy polymers (i.e., negative deviations from Henry's law at higher penetrant activities), Paul and Koros[34−37] have successfully described the sorption of gases in glassy polymers with the use of dual sorption theory. This theory suggests that penetrant molecules reside in one of two populations within the glassy matrix, where these two concurrent sorption mechanisms (regular dissolution and "hole filling") were first suggested by Barrer et al.[38] for the sorption of organic vapors in ethyl cellulose. This model has provided valuable insight into the mechanisms of small-molecule sorption in polymers in the nonequilibrium state, where this model has primarily been used to fit, but not predict, experimental data.[39−45]

More recently, Doghieri and Sarti[46−50] have developed a framework to predict the sorption of small molecules in glassy polymers: nonequilibrium thermodynamics of glassy polymers (NET-GP), which has been successfully used to predict the sorption of a number of noncondensable gases in a number of glassy polymers.[51−55] Examples of these models include the nonequilibrium lattice fluid (NELF) model[56,57] and the nonequilibrium statistical associating fluid theory (NE-SAFT),[58−60] where the NELF and NE-SAFT models incorporate both the Sanchez–Lacombe equation of state (SL-EoS) and SAFT-EoS, respectively, under a nonequilibrium thermodynamic framework. While both the NELF and NE-SAFT use residual Helmholtz energy to represent different contributions to the free energy of each component in the mixture, the NE-SAFT has an additional pure-component term that accounts for self-association due to hydrogen bonding.

Recently, the NELF model was extended to predict the sorption of water in polycarbonate[61] and PLA.[24] With no parameters in the NELF model to account for self-association of water, both the low concentration (i.e., infinite-dilution limit) of water in the glassy polymer and weak association of water molecules (i.e., dimers) were offered as explanations for the success of NELF at predicting water solubility. These initial results indicate the importance of both the absolute water concentration and states of water on the applicability of NELF in predicting water solubility. Other recent studies include the use of the perturbed-chain SAFT (PC-SAFT) model to predict the compositions of water/alcohol/poly(*N*-isopropylacrylamide) mixtures (in the equilibrium state)[62] and the use of both the nonrandom hydrogen-bonding model and the NET-GP nonrandom hydrogen-bonding model to investigate water sorption in polycaprolactone (rubbery polymer) and in a number of polyimides (glassy polymers), respectively.[63]

In this study, water sorption in PMMA was measured with a QSM at three experimental temperatures, 25, 35, and 45 °C, as a function of the external water vapor pressure. Water sorption isotherms in PMMA and in several other glassy polymers [e.g., PLA, poly(styrene) (PS), poly(vinyl chloride) (PVC), poly(ethylene terephthalate) (PET)] were predicted using two EoS-based nonequilibrium thermodynamic models: NELF and NE-SAFT. The predictions from these models were compared with water sorption data obtained from a QSM and other gravimetric techniques (data obtained from the literature). Additionally, in situ time-resolved Fourier transform infrared attenuated total reflectance (FTIR-ATR) spectroscopy was employed to study the states of water in PMMA and PLA. This spectroscopic technique provides molecular-level resolution between the glassy polymer and penetrant (water) in real time, providing critical insight into the behavior of water in the polymer (i.e., clustering due to hydrogen bonding) during the nonequilibrium sorption process.

EXPERIMENTAL SECTION

Materials. Poly(methyl methacrylate) (PMMA; M_w = 100 kg/mol, atactic beads) was purchased from Polysciences, Inc. Tetrahydrofuran (THF; anhydrous, ≥99.9%, inhibitor free) was purchased from Sigma-Aldrich. Ultrapure deionized water (resistivity ca. 16 MΩ·cm) was used for all sorption experiments.

Film Preparation. PMMA/THF solutions were produced by dissolving PMMA in THF at 5% w/w and mixing for 24 h to ensure a clear, homogeneous solution. PMMA films were fabricated by solution-casting the PMMA/THF solution onto a Teflon Petri dish to produce free-standing films for gravimetric experiments or solution-casting onto the ATR crystal surface for time-resolved FTIR-ATR spectroscopy experiments. After solution-casting onto the appropriate surface for 24 h, the PMMA films were held under vacuum for 24 h at room temperature. The films were then subsequently annealed at 70 °C under vacuum for 3 h, and then the temperature was increased to 120 °C and held under vacuum for an additional 3 h. After annealing, all PMMA films were immediately stored in a desiccator prior to sorption experiments. Immediately following each sorption experiment, the thickness of the PMMA film was measured using a digital micrometer (Mitutoyo) with a 1 μm accuracy. Each film thickness was an average of at least three individual measurements at different positions along the length of the film.

QSM. A PMMA film (ca. 50 mg), along with a metal reference (ca. 15 mg), was placed at the end of a vertical quartz spring (purchased from DeerSlayer Springs; 100 mg maximum load with 500 mm maximum extension; spring constant k_{spring} = 0.98 g/s^2), which was housed inside a temperature-controlled glass column connected to a vapor sorption apparatus.[64] The entire vapor sorption apparatus, including a glass column, along with a temperature-controlled reservoir was completely evacuated of moisture and air via vacuum for at least 2 h. After the system was completely evacuated, the valve connecting the glass column housing the quartz spring and sample to the rest of the vapor sorption apparatus was closed (leak rate less than 0.5 mmHg/day). The reservoir containing deionized water was subjected to a number of freeze–pump–thaw vacuum cycles in order to remove all dissolved gases from the liquid. Pure water vapor was then charged into the temperature-controlled reservoir at specific partial pressures, where it was allowed to equilibrate with the temperature of the

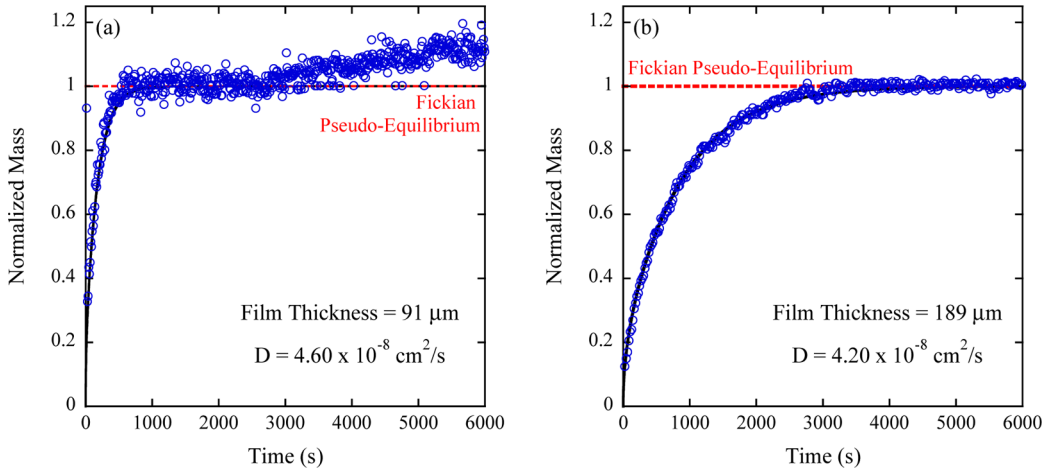

Figure 1. Water sorption kinetics in PMMA at 35 °C measured with a QSM at two different film thicknesses: (a) 91 μm; (b) 189 μm. QSM data were collected in response to an external differential change in the water vapor activity of 0.50−0.62 and 0.32−0.47 for parts a and b, respectively. Solid lines correspond to a regression to the solution of Fick's second law.[66] The dashed lines correspond to Fickian pseudoequilibrium, where the measured sorption values were determined.

jacket until steady state was reached (i.e., the pressure transducer reading was constant). Once steady state was reached, the valve separating the reservoir from the glass column was fully opened, exposing the polymer film in the glass column to a specified vapor pressure of water. The change in the extension of the spring due to water sorbing into the polymer was measured as a function of time with a high-speed charge-coupled device camera (Cognex In-Sight; series 5000, model 403; equipped with an Edmund 35 MM fixed focal length lens). The mass of water sorbed in the polymer was calculated from the spring extension data with use of the spring constant and a force balance, i.e., $F = mg = kx$. More details about this apparatus and procedures can be found elsewhere.[64]

Time-Resolved FTIR-ATR Spectroscopy. Water sorption was also measured with time-resolved IR spectroscopy using an FTIR spectrometer (Nicolet 6700 series; Thermo Electron) equipped with a horizontal, temperature-controlled ATR cell (Specac Inc.). The PMMA films were deposited on a multiple reflection, trapezoidal zinc selenide ATR crystal (Specac Inc.) with 45° beveled faces. All spectra were collected using a liquid-nitrogen-cooled mercury−cadmium−telluride detector with 32 scans per spectrum at a resolution of 2 cm^{-1}, where a spectrum was collected every 15 s. Sorption experiments were conducted at 25 °C, controlled by a temperature jacket (circulated water bath) on the ATR flow-through cell. The ATR flow-through cell was connected directly to the same vapor sorption apparatus as the QSM. Before each sorption experiment, a background spectrum of the bare ATR crystal was collected, and all subsequent collected spectra were subtracted from this spectrum. Then, a PMMA-coated ATR crystal was mounted into the ATR flow-through cell with a Kalrez gasket, and the cell was sealed. To begin each sorption experiment, the vapor sorption/ATR combined system was evacuated for at least 2 h prior to the start of each experiment (i.e., the pressure transducer reached a constant value). Then pure water vapor was charged into the vapor sorption system at a specific vapor pressure and allowed to equilibrate (i.e., the pressure transducer reading was constant). Once steady state was reached, the valve separating the ATR cell from the rest of the system was opened, allowing pure water vapor to enter the ATR cell in the space (V = 550 μL) above the polymer film (the side opposite to the polymer−crystal interface). This was followed by the collection of time-resolved IR spectra. More details regarding the apparatus and experimental procedures can be found elsewhere.[65]

RESULTS

Experimental Water Sorption in PMMA. Figure 1 shows water sorption kinetics in PMMA at 35 °C measured with a QSM after a differential change of the external water activity. Specifically, Figure 1a shows water sorption kinetics in PMMA at 35 °C with a film thickness of ca. 90 μm, where it is clear that the sorption kinetics exhibit two-stage, non-Fickian, or anomalous diffusion. Similar anomalous sorption behavior for small molecules in glassy polymers using gravimetric techniques has been previously observed,[6,67−69] where this deviation from Fickian behavior was attributed to diffusion and polymer relaxation occurring on similar time scales during the observed experimental time scale. The data in Figure 1a were normalized to the mass at the Fickian pseudoequilibrium value to help differentiate these two phenomena (water diffusion due to a concentration gradient and water diffusion induced by glassy polymer relaxation), where only relaxation-induced transport is observed at later experimental times. At longer times, the nonequilibrium state of the glassy polymer continuous to relax, allowing more water to gradually sorb into the polymer. The initial Fickian portion (early time data) of the water kinetic uptake curve can be regressed to the solution of Fick's second law[66] with only one adjustable parameter, the diffusion coefficient, where a water diffusivity of 4.60 × 10^{-8} cm^2/s was calculated. Figure 1b shows water sorption kinetics in PMMA at 35 °C for a larger film thickness of ca. 190 μm, where this deviation from Fickian diffusion was not observed over the given experimental time scale. Similar to the analysis of water sorption in the thinner film of PMMA, these data can be regressed to the solution of Fick's second law, where a water diffusivity of 4.20 × 10^{-8} cm^2/s was calculated. The water diffusivity obtained from the regression of the water sorption kinetic data falls within the range of diffusivity values reported in the literature.[21,70−73] It is worth reminding that the diffusion time is related to the polymer film thickness (L^2/D), while the relaxation time is independent of the polymer film thickness. In

dx.doi.org/10.1021/ie401713h | Ind. Eng. Chem. Res. 2013, 52, 12865−12875

other words, the experimental time scale must be extended in relation to the diffusion time in order to observe the late-time relaxation behavior, which can be clearly seen in a comparison of parts a and b of Figure 1.

This is a critical feature of small-molecule diffusion in nonequilibrium glassy polymers, where great care must be taken upon collection of sorption data, because if the polymer film thickness is large, or the measured experimental time is too short (with respect to the characteristic relaxation time of the polymer), this anomalous behavior will not be observed and sorption kinetic data collected will appear Fickian-like (see Figure 1b). Therefore, in order to use a consistent reference for comparison between samples of different thicknesses, the water sorption values reported for this system were obtained from the Fickian pseudoequilibrium portion of the kinetic data, shown by the dashed red lines in Figure 1. This type of analysis has been shown to produce consistent water solubility values between not only samples of different thicknesses but also those captured using multiple gravimetric techniques (e.g., QCM). This work, along with previous studies by Davis et al.,[24,25] highlights that the actual sorption values reported do not reflect a true equilibrium state but rather are representative of the nonequilibrium sorption of water in a glassy polymer.

Figure 2 shows water sorption isotherms in PMMA at three different experimental temperatures, 25, 35, and 45 °C,

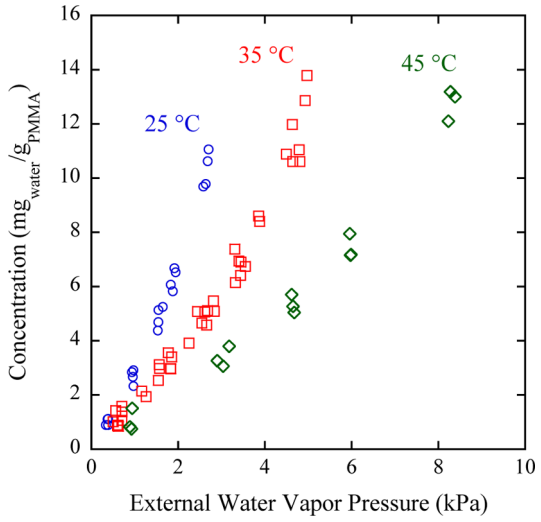

Figure 2. Water sorption isotherms in PMMA at 25, 35, and 45 °C measured with a QSM.

measured by a QSM and plotted as a function of the external water vapor pressure.

The data shown in Figure 2 were collected over a wide range water vapor activity (external vapor pressure normalized by the saturation vapor pressure), between 0.10 and 0.85, corresponding to water solubilities in PMMA spanning between ca. 0.9 and 14 mg_{water}/g_{PMMA}. These measured solubility values are lower than those previously reported at 25 °C (ca. 30% average variation)[70] but identical with those recently reported at 35 °C.[21]

Nonequilibrium Thermodynamic Prediction of Water Sorption in Glassy Polymers. Two nonequilibrium EoS-based thermodynamic models, NELF and NE-SAFT, were employed to predict the sorption isotherms of water in PMMA. Specific details regarding these models and their derivations can be found elsewhere.[24,46,55,58,74,75] Both of these nonequilibrium thermodynamic models predict sorption (i.e., mixture composition) based on pure-component data; therefore, the first step in employing these models is to obtain pure-component parameters for both the polymer (in this case, PMMA) and the penetrant (water). The SL pure-component parameters (T^*, P^*, and ρ^*) for NELF and SAFT pure-component parameters (v^{00}, m, and u^0/k) for NE-SAFT for the polymer and penetrant were obtained by fitting the pure-component data with the SL-EoS and SAFT-EoS, respectively. In the case of NE-SAFT, pressure−volume−temperature ($P\nu T$) data were used for PMMA to obtain our own pure-component SAFT parameters, while pure-component SAFT parameters for water were obtained from the literature, which were obtained by fitting both the water vapor pressure and liquid density $P\nu T$ data.[75] Pure-component SAFT parameters were also determined in this study for PLA, PAN, PET, PVC, and PC by regressing the experimental $P\nu T$ data for each polymer to the SAFT-EoS. These regressions, along with PMMA, are shown in the Supporting Information (Figures S1−S6). For the NELF model, pure-component SL parameters for PMMA and water were obtained from the literature.[53]

In addition to obtaining pure-component parameters for PMMA and water, the swelling coefficient (k) and binary-interaction parameter (K_{12} for the NELF model and k_{12} for NE-SAFT) must be determined for NELF and NE-SAFT predictions. In order to obtain an initial estimate of the swelling coefficient for water/PMMA, previous reports on density changes for PMMA films in humid environments were examined (see the Supporting Information for complete analysis).[76,77] Our analysis shows no significant changes in the predicted sorption isotherm with these small volumetric changes (<1%); therefore, the swelling coefficient was initially set at zero ($k = 0$) for all three experimental temperatures. The binary-interaction parameter was determined by regressing the model to the data at a single experimental temperature (35 °C), where the binary-interaction parameter was the only adjustable fitting parameter. This same value was then used to predict the solubility at other experimental temperatures (i.e., temperature-independent parameter). With known values of the pure-component parameters, swelling coefficient ($k = 0$), and binary-interaction parameter ($K_{12} = -0.05$ for NELF; $k_{12} = +0.006$ for NE-SAFT), the NELF and NE-SAFT models can be employed to predict the water sorption isotherm in PMMA at any temperature.

Figure 3 shows the NELF model predictions for water sorption isotherms in PMMA at 25, 35, and 45 °C, where these predictions are plotted on the same graph with the experimental data shown previously (Figure 2). As seen from Figure 3, there is good agreement between the NELF model predictions and experimental water sorption isotherms at all three temperatures, up to a water vapor activity of ca. 0.50. Above a water vapor activity of 0.50, at all three experimental temperatures, 25, 35, and 45 °C, deviation between the NELF model prediction and experimental water sorption data is clearly visible. This deviation could be due, in principle, to polymer dilation (swelling of the film) or self-association of water molecules (i.e., water clusters) that may be present at water concentration values larger than ca. 5 mg_{water}/g_{PMMA}, which could occur at these elevated water vapor activities. However, it was shown previously (see the Supporting Information) that no significant differences in the NELF model predictions were observed when PMMA dilation was included or omitted; hence, the swelling coefficient was

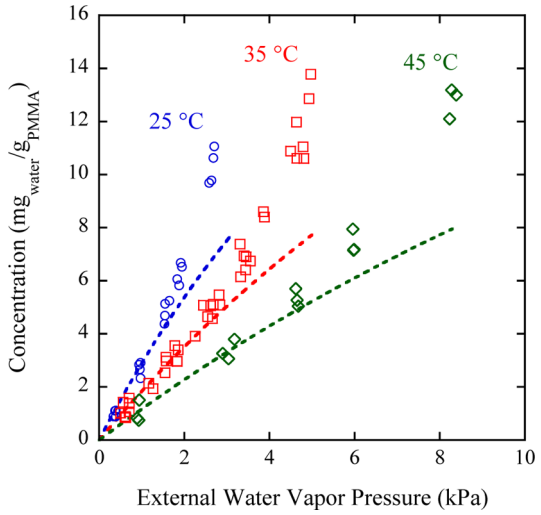

Figure 3. NELF (dashed lines) predictions of water sorption isotherms in PMMA at 25, 35, and 45 °C as a function of the external water vapor pressure. Open symbols represent experimental data obtained using a QSM.

previously set to zero. Therefore, self-association or clustering of water molecules at high water vapor activities is a more plausible reason for deviation between the model and experimental data. At high water vapor activities, the concentration of water in PMMA increases, increasing the likelihood of water molecules to self-associate and form larger, hydrogen-bonded water clusters. A similar result has been observed previously, where the NELF model was used to predict water sorption in amorphous PLA.[24] In that work, deviation between the experimental water sorption data and the NELF model was also observed, where the NELF model underpredicted water solubility in PLA at high water vapor activities (e.g., water activities above ca. 0.65). It was shown through the use of IR spectroscopy that deviation between the NELF model predictions and water sorption data was due to self-association of water molecules (i.e., water clustering) at water vapor activities above ca. 0.65. To provide further insight into the states of water in PMMA, time-resolved FTIR-ATR spectroscopy was employed over the entire water vapor activity range investigated.

Differential water sorption experiments were performed at 25 °C with time-resolved FTIR-ATR spectroscopy to complement the water/PMMA QSM experiments, where the IR spectra of the O−H stretching region of water in PMMA was investigated at each Fickian pseudoequilibrium stage after exposure to a differential step in water vapor pressure. As seen in Figure 4a, three distinguishing IR bands are present in the O−H stretching region of the spectra.

In Figure 4a, the IR band located at 3440 cm^{-1} can be attributed to an overtone of the carbonyl (C═O located at 1730 cm^{-1}) stretching from PMMA.[78] The two bands located 3550 and 3610 cm^{-1} can be attributed to two particular modes of water O−H stretching: the hydrogen-bonded O−H associated with a dimer and a free O−H bond, respectively.[79−82] The latter may represent the O−H group of a monomer or the end of a hydrogen-bonded water chain, e.g., dimer, trimer, etc. These two peaks are usually found at slightly higher wavenumbers for water alone, but these bands may be red-shifted because of the different environments (i.e., in the polymer). Other investigators have assigned these bands to symmetric and asymmetric O−H stretching of a single water molecule (i.e., monomer) that is hydrogen-bonded to two C═O groups, denoting this molecular structure as "the core of hydration".[83,84] Both of these assignments of the two IR bands located at higher wavenumbers still indicate that water exists within PMMA as either dimers or monomers (i.e., water does not strongly interact with itself). There is also a broader IR band located between 3460 and 3200 cm^{-1}, which begins to increase in intensity at water vapor activities above ca. 0.50. This IR band is representative of the stronger, hydrogen-bonded O−H stretching band associated with larger water clusters.[79] Previous investigators have observed anomalous transport of water in PMMA, where they associate this non-Fickian behavior to the formation of water clusters at higher relative water vapor pressures (water vapor activities above ca. 0.70).[8,70]

Figure 4b shows a plot of the hydrogen-bonded O−H dimer band at 3550 cm^{-1} plotted against the free O−H stretching band at 3610 cm^{-1} over the entire water vapor activity range

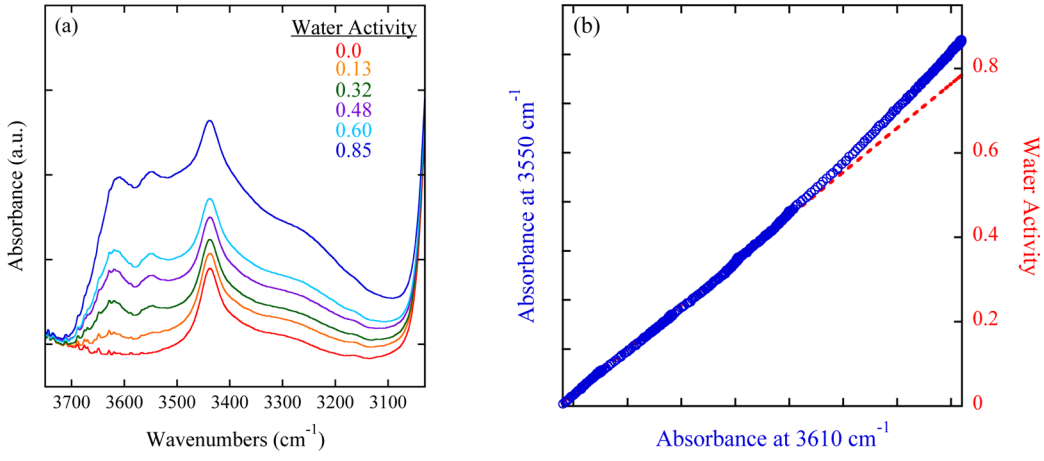

Figure 4. FTIR-ATR spectroscopy data of water in PMMA at 25 °C: (a) O−H stretching absorbance data at the Fickian pseudoequilibrium stage after exposure to several differential water vapor activity steps (numbers on graph); (b) time-resolved water O−H stretching IR absorbance (open circles) associated with the free O−H and hydrogen-bonded dimer O−H plotted against each other over the entire length of the sorption experiment. The dashed line corresponds to the 45° line.

investigated. Below a water vapor activity of ca. 0.50, a linear relationship between these two IR bands can be observed, indicating that these two IR bands are representative of the same species or state of water in PMMA; therefore, at water vapor activities below 0.50, water predominately exists in PMMA as dimers. At water vapor activities above 0.50, deviation from linearity is observed in Figure 4b. This deviation suggests that, above water vapor activities of 0.50, the two IR bands at higher wavenumbers are no longer representative of the same state of water. In particular, this means that, as the external water vapor pressure is increased, the concentration of water molecules in PMMA becomes high enough to allow for the formation of larger, hydrogen-bonded clusters of water, and therefore the free O−H band at 3610 cm^{-1} represents not only the dimer state of water but also higher water cluster sizes, e.g., hexamers.[85] This deviation from linearity observed in Figure 4b also occurs at an activity similar to that of the emergence of the broad IR band located between 3460 and 3200 cm^{-1} shown in Figure 4a, which represents the presence of larger, hydrogen-bonded clusters of water molecules in PMMA. This deviation from linearity also confirms our band assignments for 3550 and 3610 cm^{-1} (dimers at low activity and two different states of water at high activity) and calls into question previous reports that assign these bands to two different modes of the same molecule.

These IR results, specifically that water exists as dimers in PMMA below a water vapor activity of ca. 0.50 and that larger, hydrogen-bonded clusters form at activities above ca. 0.50, corroborate with the deviation observed in the NELF model predictions at water vapor activities >0.50 (see Figure 3). These results are consistent with the fact that the NELF model does not account for the strong self-association interactions of water. Similar results were observed for water sorption in PLA, another hydrophobic polymer, where deviation between the NELF model prediction and experimental sorption isotherms was observed and attributed to the formation of larger water clusters at higher water vapor activities.[24]

To account for hydrogen bonding with the introduction of water clusters in PMMA above water activities of 0.50, the NE-SAFT model was employed. As seen in Figure 5, there is excellent agreement between the NE-SAFT model predictions and experimental water sorption isotherms at all three temperatures over the entire water vapor activity range investigated. Unlike NELF, the NE-SAFT model introduces two additional pure-component parameters (ε^{AB}/k and κ^{AB}), which account for the strong self-association interactions among molecules. With the addition of these two pure-component parameters, the NE-SAFT model is able to predict the entire water sorption isotherm at all three temperatures. To our knowledge, this is the first successful attempt at predicting water solubility in a glassy polymer using NE-SAFT. The pure-component parameters for NE-SAFT for both water and PMMA are listed in Table 1.

The previous IR results (see Figure 4a) indicate why the application of NE-SAFT to model the full sorption isotherm was successful, where NE-SAFT has two additional pure-component parameters to account for self-association, i.e., hydrogen bonding, present at water vapor activities above 0.50. However, it must be noted that the NELF model prediction provides excellent agreement between the model and experimental sorption data at low water solubility values (ca. 5 mg_{water}/g_{PMMA}), where there is limited association of water molecules.

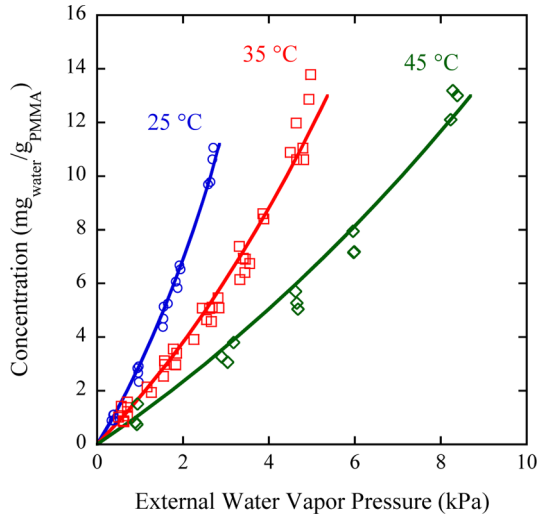

Figure 5. NE-SAFT (solid lines) predictions of water sorption isotherms in PMMA at 25, 35, and 45 °C as a function of the external water vapor pressure. Open symbols represent experimental data obtained using a QSM.

To further explore the applicability of NE-SAFT to water sorption in polymers in the nonequilibrium state, water sorption in a number of other glassy polymers was investigated. Previously, Davis et al.[24] employed the NELF model to predict water sorption in amorphous PLA at 25, 35, and 45 °C, where deviation between the NELF model and water sorption data was observed at water vapor activities above ca. 0.65. However, the NE-SAFT model prediction for water/PLA was not previously explored. Similar to the water/PMMA data in this study, the NE-SAFT model was employed here for water/PLA to determine if there is good agreement between the prediction and the data over the entire water vapor activity range. Figure 6a shows the NELF (dashed lines) and NE-SAFT (solid lines) model predictions for the sorption isotherms of water in PLA at 25, 35, and 45 °C, where these predictions are plotted on the same graph with previously measured experimental data.[24]

As seen in Figure 6a, with the additional parameters to account for associations between water molecules, the entire water sorption isotherm at 25, 35, and 45 °C can be accurately predicted using NE-SAFT. Figure 6b shows a plot of the IR band of hydrogen-bonded O−H of the dimer plotted against the IR band of the free O−H stretching, where a deviation from linearity is observed above water vapor activities of 0.65.[24] This figure is shown to highlight that, with the emergence of larger, hydrogen-bonded clusters of water at higher water vapor activities, a model that accounts for these self-association interactions must be implemented in order to properly predict the sorption behavior of water in PLA. Again, these results are similar to those observed for water sorption in PMMA (shown in Figure 4a,b), where the states of water in both of these hydrophobic glassy polymers are similar.

With excellent agreement observed between the NE-SAFT model predictions and experimental water sorption data obtained for PMMA and PLA, the NE-SAFT model was extended to predict the water sorption behavior in other glassy polymers. The results of this analysis are shown in Figure 7, where water sorption data were obtained from the literature.[21,86,87]

As seen in Figure 7 and similar to the results observed for water/PMMA and water/PLA, there is excellent agreement

Table 1. Pure-Component NE-SAFT Model Parameters for Water and PMMA

substance	ρ [g/cm^3]	v^{00} [L/kmol]	m^b	u^0/k [K]	e_{ii}	no. of sites	ε^{AB}/k [K]	κ^{AB}
water[a]	0.997	10.0	1.179	528.17	1.0	2	1809.0	0.01593
PMMA	1.20	11.600	4249	373.00	10.0	0		

[a]Pure-component parameters obtained from Huang and Radosz.[74] [b]The molecular weight is 100 kg/mol.

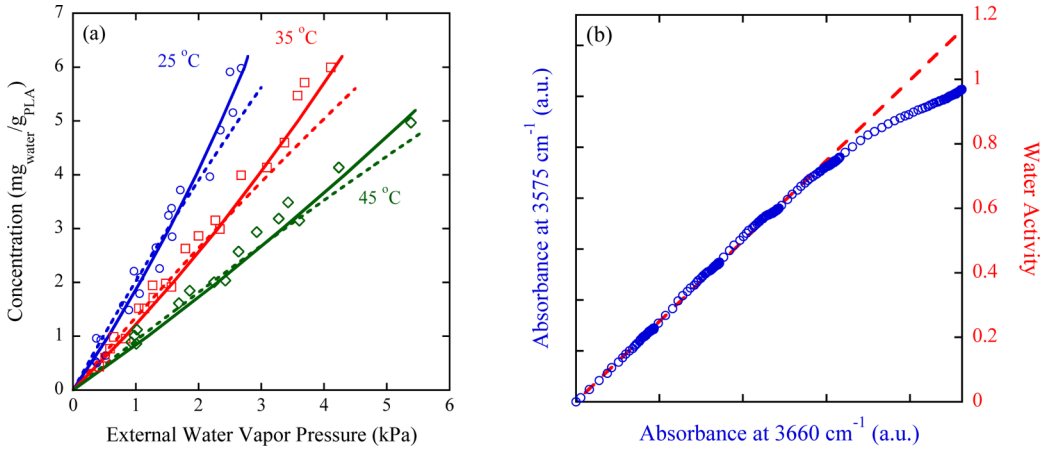

Figure 6. (a) NELF (dashed lines) and NE-SAFT (solid lines) model predictions of the water sorption isotherms in PLA at 25, 35, and 45 °C as a function of the external water vapor pressure. Open symbols represent experimental data obtained using a QSM. (b) Time-resolved water O−H stretching IR absorbance (open circles) associated with the free O−H dimer and hydrogen-bound O−H plotted against each other over the entire sorption experimental time at 35 °C. The dashed line corresponds to the 45° line. Water sorption data and NELF model predictions in parts a and b were reproduced from ref 24.

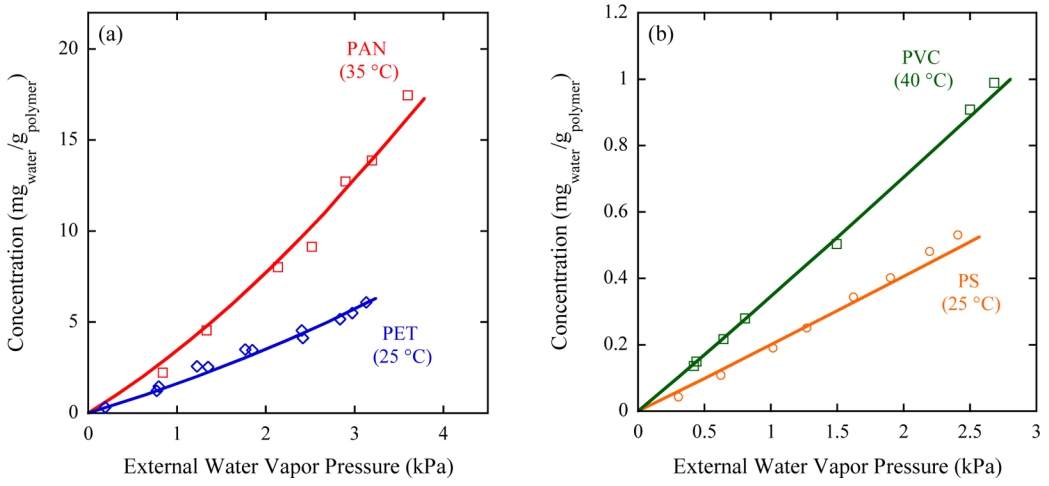

Figure 7. NE-SAFT model predictions (solid lines) and experimental water sorption data (open symbols) for (a) PAN and PET and (b) PVC and PS. Experimental water sorption data were obtained from refs 21, 86, and 87.

between the NE-SAFT model predictions and experimental water sorption data for these additional four glassy polymers. The pure-component parameters for the glassy polymers investigated are listed in Table 2 (binary-interaction parameters can be found in Supporting Information Figure S1).

The results shown here highlight the applicability of the NE-SAFT model to accurately predict water sorption in hydrophobic glassy polymers. Note that for the case when water solubility values are significantly low, as evidenced by a relatively linear relationship between the water solubility and external water vapor pressure (e.g., water in PC and PVC; see Figure 7b), the ability of the NELF model to predict the data may be adequate. However, the NELF model provides a less physically accurate representation of the sorption process compared to NE-SAFT, where the strong self-associating interactions that are present in hydrogen-bound water clusters are absent from this model. Ideally, the ability to predict water

Table 2. Pure-Component NE-SAFT Model Parameters for a Number of Glassy Polymers

substance	ρ [g/cm^3]	v^{00} [L/kmol]	m^a	u^0/k [K]	e_{ii}	no. of sites
PLA	1.240	11.400	4145	312.00	10.0	0
PS	1.045	26.000	2569	501.25	10.0	0
PAN	1.184	11.570	4716	584.25	10.0	0
PET	1.389	11.045	3963	441.70	10.0	0
PVC	1.381	10.120	4165	362.05	10.0	0

[a]The molecular weight for all polymers is 100 kg/mol, except PS, where the molecular weight is 110 kg/mol.

dx.doi.org/10.1021/ie401713h | Ind. Eng. Chem. Res. 2013, 52, 12865−12875

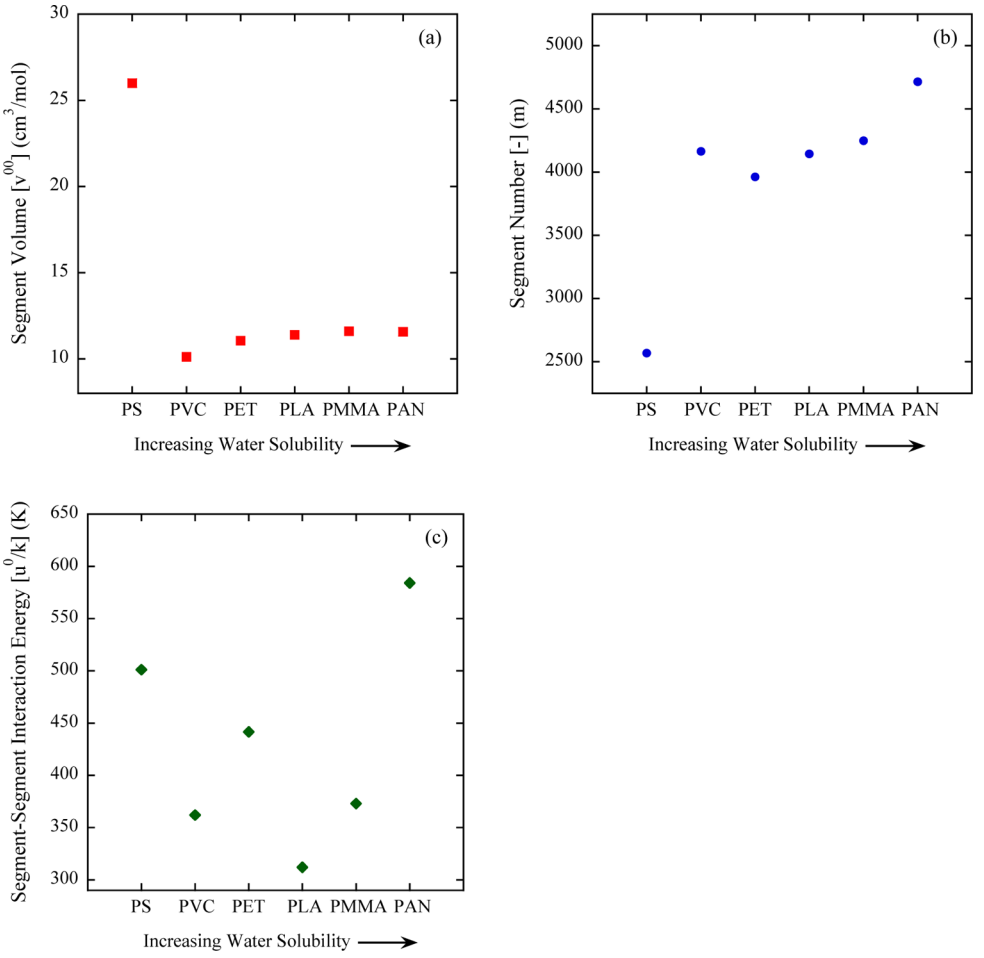

Figure 8. Pure-component polymer SAFT parameters (a) segment volume, (b) segment number, and (c) segment−segment interaction energy, plotted against each glassy polymer in order of increasing water solubility.

solubility values in glassy polymers, through correlations between pure-component parameters and water solubility, could aid in the design of new glassy polymers as moisture-barrier materials. In order to elucidate whether the pure-component parameters obtained from NE-SAFT correlate to absolute water solubility in these glassy polymers, these parameters (segment volume, segment number, and segment−segment interaction energy) were plotted for each glassy polymer (listed in order of increasing water solubility) and are shown in Figure 8.

Shown in Figure 8b, the segment number increases with increasing water solubility. There appears to be no discernible correlation between the segment−segment interaction energy and water uptake in the glassy polymers investigated, which is somewhat surprising because it is well accepted that enthalpic contributions play a large role in how different fluids behave in mixtures. The observed correlation between the segment number and absolute water solubility (Figure 8b) is interesting because this parameter influences the geometry of each polymer segment and, in turn, the packing of the polymer chains. The segment number can be related to the amount in which a material deviates from spherical symmetry. Similar to the acentric factor (ω)[88] in thermodynamics, which is a measure of the sphericalness of molecules ($\omega \sim 0$ for spherical molecules like argon, neon, and methane), the segment number, m, is ~1 for these same spherical molecules (e.g., m is ~1 for methane).[89−91] Therefore, as the segment number, m, increases, the segments of these polymer chains deviate further from "ideal" spheres (e.g., methane) and begin to behave more like rods (segments with high aspect ratios, L/D).

Previous research has shown that the packing density of spherical systems ($f \sim 0.64$) is higher than that of rodlike systems, where the packing densities can drop significantly (from $f \sim 0.32$ to 0.18).[92,93] Physically, this decrease in the packing density equates to an increase in the free volume (void space) of the system. Applying these physics to the glassy polymers in this study implies that increases in the segment number lead to a higher fraction of trapped free volume within the polymer in a nonequilibrium state due to the irregular (random) packing of the nonspherical polymer segments. With increases in the polymer free volume, the solubility of water increases because there is more unoccupied space for water molecules to sorb. This physical phenomenon explains the observed relationship between the segment number and water solubility observed in Figure 8b. Decreases in the penetrant solubility with decreases in the polymer free volume are well established in the literature.[94,95] Although pure-component SAFT parameters do not account for additional constraints in polymers (e.g., chain entanglements), these results (Figure 8b) preliminarily suggest that this analysis can be used in the future to correlate water sorption to pure-component parameters in other (current) or newly synthesized glassy polymers.

CONCLUSIONS

This work demonstrates the ability of nonequilibrium thermodynamics, specifically NELF and NE-SAFT, to accurately predict water sorption in six glassy polymers, including PMMA, PLA, PAN, PET, PVC, and PS. Specifically, good agreement between the NELF model prediction and experimental data in PMMA was only observed at water activities <0.50, while NE-SAFT provided excellent predictions of the water sorption isotherms at all three temperatures over the entire water vapor activity range explored. In situ time-resolved FTIR-ATR spectroscopy was employed to investigate the states of water present in PMMA during the sorption process, where the association (clustering) of water molecules at elevated water activities was observed. This observation provides a rationale for deviation between the NELF model and water/PMMA experimental data, where the association of water molecules is not accounted for in the NELF model. In contrast, NE-SAFT contains two additional pure-component terms to account for this observed association of water molecules, and consequently the model provides an accurate prediction of the entire water sorption isotherm in PMMA. These results were similarly reproduced for water in PLA, where similar water behavior compared to PMMA was observed. NE-SAFT analysis was extended to other glassy polymers, including PAN, PET, PVC, and PS, where excellent agreement between NE-SAFT and the experimental data was also observed. Furthermore, a correlation between the SAFT pure-component polymer parameter, segment number, was observed and could be utilized as a scaling parameter for water sorption behavior in other or newly synthesized glassy polymers for moisture-barrier applications.

ASSOCIATED CONTENT

Supporting Information

NE-SAFT pure-component and binary-interaction parameters and swelling coefficient determination. This material is available free of charge via the Internet at http://pubs.acs.org.

AUTHOR INFORMATION

Corresponding Author

*E-mail: elabd@drexel.edu. Tel: +1 215 895 0986. Fax: +1 215 895 5837.

Notes

The authors declare no competing financial interest.

ACKNOWLEDGMENTS

The authors acknowledge financial support of the National Science Foundation (CAREER 0644593) and the United States Department of Agriculture and United States Department of Energy (Grant 06GO96002).

REFERENCES

(1) Langer, R. S.; Peppas, N. A. Present and future applications of biomaterials in controlled drug delivery systems. *Biomaterials* **1981**, *2*, 201−214.

(2) Cath, T. Y.; Childress, A. E.; Elimelech, M. Forward osmosis: Principles, applications, and recent developments. *J. Membr. Sci.* **2006**, *281*, 70−87.

(3) Geise, G. M.; Lee, H.-S.; Miller, D. J.; Freeman, B. D.; McGrath, J. E.; Paul, D. R. Water Purification by Membranes: The Role of Polymer Science. *J. Polym. Sci., Part B: Polym. Phys.* **2010**, *48*, 1685−1718.

(4) Mauritz, K. A.; Moore, R. B. State of Understanding of Nafion. *Chem. Rev.* **2004**, *104*, 4535−4585.

(5) Yang, Z.; Zhang, J.; Kintner-Meyer, M. C. W.; Lu, X.; Choi, D.; Lemmon, J. P.; Liu, J. Electrochemical Energy Storage for Green Grid. *Chem. Rev.* **2011**, *111*, 3577−3613.

(6) van der Wel, G. K.; Adan, O. C. G. Moisture in organic coatings − a review. *Prog. Org. Coat.* **1999**, *37*, 1−14.

(7) Auras, R.; Harte, B.; Selke, S. An Overview of Polylactides as Packaging Materials. *Macromol. Biosci.* **2004**, *4*, 835−864.

(8) Connelly, R. W.; McCoy, N. R.; Koros, W. J.; Hopfenberg, H. B.; Stewart, M. E. The Effect of Sorbed Penetrants on the Aging of Previously Dilated Glassy Polymer Powders. I. Lower Alcohol and Water Sorption in Poly(methyl Methacrylate). *J. Appl. Polym. Sci.* **1987**, *34*, 703−719.

(9) Del Nobile, M. A.; Mensitieri, G.; Netti, P. A.; Nicolais, L. Anomalous Diffusion in Poly-Ether-Ether-Ketone. *Chem. Eng. Sci.* **1994**, *49*, 633−644.

(10) Frisch, H. L. Sorption and Transport in Glassy Polymers—A Review. *Polym. Eng. Sci.* **1980**, *20*, 2−13.

(11) Hernandez, R. J.; Gavara, R. Sorption and Transport of Water in Nylon-6 Films. *J. Polym. Sci., Part B: Polym. Phys.* **1994**, *32*, 2367−2374.

(12) Schult, K. A.; Paul, D. R. Techniques for Measurement of Water Vapor Sorption and Permeation in Polymer Films. *J. Polym. Sci., Part B: Polym. Phys.* **1996**, *61*, 1865−1876.

(13) Schult, K. A.; Paul, D. R. Water Sorption and Transport in a Series of Polysulfones. *J. Polym. Sci., Part B: Polym. Phys.* **1996**, *34*, 2805−2817.

(14) Schult, K. A.; Paul, D. R. Water Sorption and Transport in Blends of Polyethyloxazoline and Polyethersulfone. *J. Polym. Sci., Part B: Polym. Phys.* **1997**, *35*, 993−1007.

(15) Schult, K. A.; Paul, D. R. Water Sorption and Transport in Blends of Poly(vinyl pyrrolidone) and Polysulfone. *J. Polym. Sci., Part B: Polym. Phys.* **1997**, *35*, 655−674.

(16) Chang, M.-J.; Myerson, A. S.; Kwei, T. K. The Effect of Hydrogen Bonding on Vapor Diffusion in Water-Soluble Polymers. *J. Appl. Polym. Sci.* **1997**, *66*, 279−291.

(17) Rivin, D.; Kendrick, C. E.; Gibson, P. W.; Schneider, N. S. Solubility and transport behavior of water and alcohols in Nafion. *Polymer* **2001**, *42*, 623−635.

(18) Kelkar, A. J.; Paul, D. R. Water vapor transport in a series of polyarylates. *J. Membr. Sci.* **2001**, *181*, 199−212.

(19) Fu, H.; Jia, L.; Xu, J. Studies on the Sulfonation of Poly(phenylene oxide) (PPO) and Permeation Behavior of Gases and Water Vapor Through Sulfonated PPO Membranes: II. Permeation Behavior of Gases and Water Vapor Through Sulfonated PPO Membranes. *J. Appl. Polym. Sci.* **1994**, *51*, 1405−1409.

(20) Du, A.; Koo, D.; Theryo, G.; Hillmyer, M. A.; Cairncross, R. A. Water transport and clustering behavior in homopolymer and graft copolymer polylactide. *J. Membr. Sci.* **2012**, *396*, 50−56.

(21) Rodrígez, O.; Fornasiero, F.; Arce, A.; Radke, C. J.; Prausnitz, J. M. Solubilities and diffusivities of water vapor in poly-(methylmethacrylate), poly(2-hydroxyethylmethacrylate), poly(*N*-vinyl-2-pyrrolidone) and poly(acrylonitrile). *Polymer* **2003**, *44*, 6323−6333.

(22) Arce, A.; Fornasiero, F.; Rodrígez, O.; Radke, C. J.; Prausnitz, J. M. Sorption and transport of water vapor in thin polymer films at 35 °C. *Phys. Chem. Chem. Phys.* **2004**, *6*, 103−108.

(23) Zimm, B. H.; Lundberg, J. L. Sorption of Vapors By High Polymers. *J. Chem. Phys.* **1956**, *60*, 425−428.

(24) Davis, E. M.; Minelli, M.; Giancinti Baschetti, M.; Sarti, G. C.; Elabd, Y. A. Nonequilibrium Sorption of Water in Polylactide. *Macromolecules* **2012**, *45*, 7486−7494.

(25) Davis, E. M.; Minelli, M.; Giacinti Baschetti, M.; Elabd, Y. A. Non-Fickian Diffusion of Water in Polylactide. *Ind. Eng. Chem. Res.* **2013**, *52*, 8664−8673.

(26) Flory, P. J. *Principles in Polymer Chemistry*; Cornell University Press: Ithaca, NY, 1953.

(27) Flory, P. J. Thermodynamics of High Polymer Solutions. *J. Chem. Phys.* **1941**, *9*, 660−661.
(28) Flory, P. J. Thermodynamics of High Polymer Solutions. *J. Chem. Phys.* **1942**, *10*, 51−61.
(29) Huggins, M. L. Solutions of Long Chain Compounds. *J. Chem. Phys.* **1941**, *9*, 440.
(30) Hancock, B. C.; Zografi, G. The Use of Solution Theories for Predicting Water Vapor Absorption by Amorphous Pharmaceutical Solids: A Test of the Flory−Huggins and Vrentas Models. *Pharm. Res.* **1993**, *10*, 1262−1267.
(31) Zhang, J.; Zografi, G. The Relationship between "BET" and Free Volume-Derived Models for Water Vapor Absorption by Amorphous Solids. *J. Pharm. Sci.* **2000**, *89*, 1063−1072.
(32) Lim, L.-T.; Britt, I. J.; Tung, M. A. Sorption and Transport of Water Vapor in Nylon 6,6 Film. *J. Appl. Polym. Sci.* **1999**, *71*, 197−206.
(33) Cornejo-Bravo, J. M.; Siegel, R. A. Water vapour sorption behaviour of copolymers of *N*,*N*-diethylaminoethyl methacrylate and methyl methacrylate. *Biomaterials* **1996**, *17*, 1187−1193.
(34) Koros, W. J.; Chan, A. H.; Paul, D. R. Sorption and Transport of Various Gases in Polycarbonate. *J. Membr. Sci.* **1977**, *2*, 165−190.
(35) Paul, D. R.; Koros, W. J. Effect of Partially Immobilizing Sorption on Permeability and the Diffusion Time Lab. *J. Polym. Sci., Polym. Phys. Ed.* **1976**, *14*, 675−685.
(36) Koros, W. J.; Paul, D. R.; Rocha, A. A. Carbon Dioxide Sorption and Transport in Polycarbonate. *J. Polym. Sci., Polym. Phys. Ed.* **1976**, *14*, 687−702.
(37) Koros, W. J.; Paul, D. R. CO_2 Sorption and Poly(ethylene Terephthalate) above and below the Glass Transition. *J. Polym. Sci., Polym. Phys. Ed.* **1978**, *16*, 1947−1963.
(38) Barrer, R. M.; Barrie, J. A.; Slater, J. Sorption and Diffusion in Ethyl Cellulose. Part III. Comparison between Ethyl Cellulose and Rubber. *J. Polym. Sci.* **1958**, *27*, 177−197.
(39) Masi, P.; Paul, D. R.; Barlow, J. W. Gas Sorption and Transport in a Copolyester and Its Blend with Polycarbonate. *J. Polym. Sci., Polym. Phys. Ed.* **1982**, *20*, 15−26.
(40) Huvard, G. S.; Stannett, V. T.; Koros, W. J.; Hopfenberg, H. B. The Pressure Dependence of CO_2 Sorption and Permeation in Poly(Acrylonitrile). *J. Membr. Sci.* **1980**, *6*, 185−201.
(41) Felder, R. M.; Patton, C. J.; Koros, W. J. Dual-Mode Sorption and Transport of Sulfur Dioxide in Kapton Polyimide. *J. Polym. Sci., Polym. Phys. Ed.* **1981**, *19*, 1895−1909.
(42) Barrie, J. A.; Williams, M. J. L.; Munday, K. Sorption and Diffusion of Hydrocarbon Vapors in Glassy Polymers. *Polym. Eng. Sci.* **1980**, *20*, 20−29.
(43) Muruganandam, N.; Koros, W. J.; Paul, D. R. Gas Sorption and Transport in Substituted Polycarbonates. *J. Polym. Sci., Part B: Polym. Phys.* **1987**, *25*, 1999−2026.
(44) Kirchheim, R. Sorption and Partial Molar Volume of Small Molecules in Glassy Polymers. *Macromolecules* **1992**, *25*, 6952−6960.
(45) Story, B. J.; Koros, W. J. Sorption and transport of CO_2 and CH_4 in chemically modified poly(phenylene oxide). *J. Membr. Sci.* **1992**, *67*, 191−210.
(46) Doghieri, F.; Sarti, G. C. Nonequilibrium Lattice Fluids: A Predictive Model for the Solubility in Glassy Polymers. *Macromolecules* **1996**, *29*, 7885−7896.
(47) De Angelis, M. G.; Sarti, G. C.; Doghieri, F. Correlations between Penetrant Properties and Infinite Dilution Gas Solubility in Glassy Polymers: NELF Model Derivation. *Ind. Eng. Chem. Res.* **2007**, *46*, 7645−7656.
(48) Carlà, V.; Hussain, Y.; Grant, C.; Sarti, G. C.; Carbonell, R. G.; Doghieri, F. Modeling Sorption Kinetics of Carbon Dioxide in Glassy Polymeric Films Using the Nonequilibrium Thermodynamics Approach. *Ind. Eng. Chem. Res.* **2009**, *48*, 3844−3854.
(49) Doghieri, F.; Ghedini, M.; Quinzi, M.; Rethwisch, D. G.; Sarti, G. C. In *Advanced Materials for Membrane*; Pinnau, I., Freeman, B. D., Eds.; ACS Symposium Series 876; American Chemical Society: Washington, DC, 2004; pp 55−73.
(50) Carlà, V.; Wang, K.; Hussain, Y.; Efimenko, K.; Genzer, J.; Grant, C.; Sarti, G. C.; Carbonell, R. G.; Doghieri, F. Nonequilibrium Model for Sorption and Swelling of Bulk Glassy Polymer Films with Supercritical Carbon Dioxide. *Macromolecules* **2005**, *38*, 10299−10313.
(51) Giacinti Baschetti, M.; Doghieri, F.; Sarti, G. C. Solubility in Glassy Polymers: Correlations through the Nonequilibrium Lattice Fluid Model. *Ind. Eng. Chem. Res.* **2001**, *40*, 3027−3037.
(52) Bonavoglia, B.; Storti, G.; Morbidelli, M. Modeling of the Sorption and Swelling Behavior of Semicrystalline Polymers in Supercritical CO_2. *Ind. Eng. Chem. Res.* **2006**, *45*, 1183−1200.
(53) De Angelis, M. G.; Sarti, G. C.; Doghieri, F. NELF model prediction of the infinite dilution gas solubility in glassy polymers. *J. Membr. Sci.* **2007**, *289*, 106−122.
(54) De Angelis, M. G.; Sarti, G. C. Solubility and Diffusivity of Gases in Mixed Matrix Membranes Containing Hydrophobic Fumed Silica: Correlations and Predictions Based on the NELF Model. *Ind. Eng. Chem. Res.* **2008**, *47*, 5214−5226.
(55) De Angelis, M. G.; Merkel, T. C.; Bondar, V. I.; Freeman, B. D.; Doghieri, F.; Sarti, G. C. Gas Sorption and Dilation in Poly(2,2-bistrifluoromethyl-4,5-difluoro-1,3-dioxole-*co*-tetrafluoroethylene): Comparison of Experimental Data with Predictions of the Non-equilibrium Lattice Fluid Model. *Macromolecules* **2002**, *35*, 1276−1288.
(56) Sarti, G. C.; Doghieri, F. Predictions of the solubility of gases in glassy polymers based on the NELF model. *Chem. Eng. Sci.* **1998**, *53*, 3435−3447.
(57) Doghieri, F.; Sarti, G. C. Predicting the low pressure solubility of gases and vapors in glassy polymers by the NELF model. *J. Membr. Sci.* **1998**, *147*, 73−86.
(58) Chapman, W. G.; Gubbins, K. E.; Jackson, G.; Radosz, M. SAFT: Equation-of-State Solution Model for Associating Fluids. *Fluid Phase Equilib.* **1989**, *52*, 31−38.
(59) De Angelis, M. G.; Doghieri, F.; Sarti, G. C.; Freeman, B. D. Modeling gas sorption in amorphous Teflon through the non equilibrium thermodynamics for glassy polymers (NET-GP) approach. *Desalination* **2006**, *193*, 82−89.
(60) Doghieri, F.; Ghedini, M.; Quinzi, M.; Rethwisch, D.; Sarti, G. C. Gas solubility in glassy polymers: predictions from non-equilibrium EoS. *Desalination* **2002**, *144*, 73−78.
(61) Sarti, G. C.; De Angelis, M. G. Calculation of the Solubility of Liquid Solutes in Glassy Polymers. *AIChE J.* **2012**, *58*, 292−301.
(62) Arndt, M. C.; Sadowski, G. Modeling Poly(*N*-isopropylacrylamide) Hydrogels in Water/Alcohol Mixtures with PC-SAFT. *Macromolecules* **2012**, *45*, 6686−6696.
(63) Scherillo, G.; Galizia, M.; Musto, P.; Mensitieri, G. Water Sorption Thermodynamics in Glassy and Rubbery Polymers: Modeling the Interactional Issues Emerging from FTIR Spectroscopy. *Ind. Eng. Chem. Res.* **2013**, *52*, 8674−8691.
(64) Elabd, Y. A.; Barbari, T. A. Separating Solvation from Molecular Diffusion in Polymers. *AIChE J.* **2001**, *47*, 1255−1262.
(65) Hallinan, D. T., Jr.; Elabd, Y. A. Diffusion of Water in Nafion Using Time-Resolved Fourier Transform Infrared-Attenuated Total Reflectance Spectroscopy. *J. Phys. Chem. B* **2009**, *113*, 4257−4266.
(66) Crank, J. *Mathematics of Diffusion*, 2nd ed.; Wiley: New York, 2003.
(67) Neogi, P. Part II: Anomalous Sorption. *AIChE J.* **1983**, *29*, 833−839.
(68) Berens, A. R.; Hopfenberg, H. B. Diffusion and relaxation in glassy polymer powders: 2. Separation of diffusion and relaxation parameters. *Polymer* **1978**, *19*, 489−496.
(69) Huang, S. J.; Durning, C. J.; Freeman, B. D. Modeling weakly non-linear two-stage sorption kinetics in glassy polymer films. *J. Membr. Sci.* **1998**, *143*, 1−11.
(70) Roussis, P. P. Diffusion of Water Vapour in Polymethyl Methacrylate. *J. Membr. Sci.* **1983**, *15*, 141−155.
(71) Barrie, J. A.; Machin, D. Diffusion and Association of Water in Some Polyalkylmethacrylates. *Trans. Faraday Soc.* **1971**, *67*, 244−256.
(72) Bueche, F. Diffusion of Water in Polymethyl Methacrylate. *J. Polym. Sci.* **1954**, *14*, 414−416.

(73) Hsu, W. P.; Li, R. J.; Myerson, A. S.; Kwei, T. K. Sorption and diffusion of water vapour in hydrogen-bonded polymer blends. *Polymer* **1993**, *34*, 597−603.
(74) Huang, S. H.; Radosz, M. Equation of State for Small, Large, Polydisperse, and Associating Molecules: Extension to Fluid Mixtures. *Ind. Eng. Chem. Res.* **1991**, *30*, 1994−2005.
(75) Huang, S. H.; Radosz, M. Equations of State for Small, Large, Polydisperse, and Associating Molecules. *Ind. Eng. Chem. Res.* **1990**, *29*, 2284−2294.
(76) Kimmel, R. M.; Uhlmann, D. R. Effects of High Pressure on Amorphous Polymers: Densification of Polymethyl Methacrylate. *J. Appl. Phys.* **1970**, *41*, 2917−2927.
(77) Turner, D. T. Polymethyl methacrylate plus water: sorption kinetics and volumetric changes. *Polymer* **1982**, *23*, 197−202.
(78) Willis, H. A.; Zichy, V. J. I.; Hendra, P. J. The Laser-Raman and Infrared Spectra of Poly(Methyl Methacrylate). *Polymer* **1969**, *10*, 737−746.
(79) Scatena, L. F.; Brown, M. G.; Richmond, G. L. Water at Hydrophobic Surfaces: Weak Hydrogen Bonding and Strong Orientation Effects. *Science* **2001**, *292*, 908−912.
(80) Du, Q.; Superfine, R.; Freysz, E.; Shen, Y. R. Vibrational Spectroscopy of Water at the Vapor/Water Interface. *Phys. Rev. Lett.* **1993**, *70*, 2313−2316.
(81) Buck, U.; Huisken, F. Infrared Spectroscopy of Size-Selected Water and Methanol Clusters. *Chem. Rev.* **2000**, *100*, 3863−3890.
(82) Paul, J. B.; Collier, C. P.; Saykally, R. J.; Scherer, J. J.; O'Keefe, A. Direct Measurement of Water Cluster Concentration by Infrared Cavity Ringdown Laser Absorption Spectroscopy. *J. Phys. Chem. A* **1997**, *101*, 5211−5214.
(83) Iwamoto, R.; Matsuda, T. Infrared and Near-Infrared Spectral Evidence for Water Clustering in Highly Hydrated Poly(methyl Methacrylate). *Anal. Chem.* **2007**, *79*, 3455−3461.
(84) Iwamoto, R.; Matsuda, T. Interaction of Water in Polymers: Poly(ethylene-*co*-vinyl acetate) and Poly(vinyl acetate). *J. Polym. Sci., Part B: Polym. Phys.* **2005**, *43*, 777−785.
(85) Pérez, C.; Muckle, M. T.; Zaleski, D. P.; Seifert, N. A.; Temelso, B.; Shields, G. C.; Kisiel, Z.; Pate, B. H. Structures of Cage, Prism, and Book Isomers of Water Hexamer from Broadband Rotational Spectroscopy. *Science* **2012**, *336*, 897−901.
(86) Yasuda, H.; Stannett, V. Permeation, Solution, and Diffusion of Water in Some High Polymers. *J. Polym. Sci.* **1962**, *57*, 907−923.
(87) Day, A. G. Water Sorption in Dielectrics. *Trans. Faraday Soc.* **1963**, *59*, 1218−1224.
(88) Elliot, J. R.; Lira, C. T. *Introductory Chemical Engineering Thermodynamics*, 1st ed.; Prentice Hall: Upper Saddle River, NJ, 1999.
(89) Voutsas, E. C.; Boulougouris, G. C.; Economou, I. G.; Tassios, D. P. Water/Hydrocarbon Phase Equilibria Using the Thermodynamic Perturbation Theory. *Ind. Eng. Chem. Res.* **2000**, *39*, 797−804.
(90) Pàmies, J. C.; Vega, L. F. Vapor−Liquid Equilibria and Critical Behavior of Heavy *n*-Alkanes Using Transferable Parameters from the Soft-SAFT Equation of State. *Ind. Eng. Chem. Res.* **2001**, *40*, 2532−2543.
(91) Nguyen-Huynh, D.; Tran, T. K. S.; Tamouza, S.; Passarello, J. P.; Tobaly, P.; de Hemptinne, J. C. Modeling Phase Equilibria of Asymmetric Mixtures Using a Group-Contribution SAFT (GC-SAFT) with a kij Correlation Method Based on London's Theory. 2. Application to Binary Mixtures Containing Aromatic Hydrocarbons, *n*-Alkanes, CO_2, N_2, and H_2S. *Ind. Eng. Chem. Res.* **2008**, *47*, 8859−8868.
(92) Brouwers, H. J. H. Particle-size distribution and packing fraction of geometric random packings. *Phys. Rev. E* **2006**, *74*, 031309(1−14).
(93) Philipse, A. P. The Random Contact Equation and Its Implications for (Colloidal) Rods in Packings, Suspensions, and Anisotropic Powders. *Langmuir* **1996**, *12*, 1127−1133.
(94) Shah, V. M.; Hardy, B. J.; Stern, S. A. Solubility of Carbon Dioxide, Methane, and Propane in Silicone Polymers. Effect of Polymer Backbone Chains. *J. Polym. Sci., Part B: Polym. Phys.* **1993**, *31*, 313−317.
(95) Berens, A. R. The Solubility of Vinyl Chloride in Poly(Vinyl Chloride). *Angew. Makromol. Chem.* **1975**, *47*, 97−110.